



## Weldability of New Material Sandwich Steel for Automotive Applications

**Ihsan Kadhom Abbas Al Naimi**

*Vocational Education/ Ministry of Education*

E-mail: [Ihsan\\_kad@yahoo.com](mailto:Ihsan_kad@yahoo.com)

(Received 17 May 2015; accepted 28 October 2015)

### Abstract

Today, the world is faced with an energy crisis because of a continuous increasing consumption of fuels due to the increasing demand for all types of vehicles. This study is one of the efforts dealing with reducing the weight of vehicles by using a new material of sandwich steel, which consists of two skin steel sheets with a core of a polymer material. Resistance spot welding (RSW) can be easily implemented on metals; however, a copper shunt tool was designed to perform the resistance welding of sandwich steel with DP800 cover sheets to resolve a non-conductivity problem of a polymer core. Numerical simulations with SORPAS<sup>®</sup>3D were employed to test the weldability of this new material and supported by many practical experiments. In conclusion, it was found that the weldability could be improved with using two pulses and optimizing their welding parameters. Tensile-shearing tests were carried out to evaluate the strength of welding sheets. Macro/micrograph and SEM/EDS examinations were also carried out to analyze the welding area and compare the nugget of welding sheets with different welding parameters. The concluded optimum welding parameters are: 3.5 kN, (5.5 kA, 8 cycles), and (10 kA, 5 cycles) for the electrode force, welding current and time of first and second pulse respectively.

**Keywords:** Sandwich steel, DP800, RSW, Weldability, Shunt tool, SORPAS<sup>®</sup>3D.

### 1. Introduction

As long as there is ongoing increasing demand of vehicles with all types, thus increasing fossil fuels consumption leading to real problems of pollution and global warming, scientists and automakers continue research on light materials to reduce fuel consumption and CO<sub>2</sub> emission as well as preserving the safety requirements, functionality and comfort in these vehicles. Therefore, it is essential to find cost-effective solutions to these issues. One of these solutions is to use aluminum alloy sheets in the automobile industry; however, the cost of these metals is still high as well as the productivity of resistance spot welding aluminum is lower than steel [1-4].

RSW is a key technology in automotive assembly production. Modern small vehicles contain (2000-5000) spot welds [5]. The process is very fast, low cost, minimum skill labor

requirements, easily automated [6 and 7], and can weld many different material combinations that are difficult or even impossible to join by other welding techniques [8]. It is also suitable for small batch production, because the method is flexible, equipment simple and the welding process is easy to control. The process is also applied in the manufacture of other transportation, household appliance manufacturers, and more. The most important adjustable RSW parameters are welding current, welding time, electrode force, and electrode geometry and its materials. The other adjustable parameters include the duration of squeeze and hold time, possible heat treatments before or after welding (pre/post weld), adjustment of the up-and-downslope of the welding current (slope function), changes in electrode force and timing on the basis of work stage. In addition, the pulsation of welding current which was used in this work. However, accurate control and synchronization of current and

electrode force is required for the process to get sound weldment [9].

In order to prevent noise and vibration from transmission as well as reducing weight, vibration damping steel sheets (VDSS) which are composed of two steel-sheet skin layers and a viscoelastic polymer resin layer have been developed by steelmakers and has been commercially available since 1950. However, it is rarely used in high volume applications, such as those in the automotive industry [10]. The vibration damping steel sheets, however, must carry out spot welding by providing a bypass circuit, because polymer resin is electrical insulator. Therefore, with parts requiring many weld spots, it is a difficult matter to carry out spot welding to provide a bypass circuit for every weld point. Akihiko Nishimoto and et.al. (1988) in NKK a Japanese industries company developed the weldable VDSS sheets which can be welded without the aid of bypass circuit device by adding nickel particles to the resin layer to solve the non-conductivity of the resin. They also analyzed many other particles additives to the resin such; Fe, Al, Cu, Sn, Zn, and graphite with different size particles, and they concluded; nickel particles with size (44-74  $\mu\text{m}$ ) most optimum particles to make the VDSS spot weldable even with 5 wt.% [11]. Furthermore, other researchers investigated the weldable of VDSS by the addition of filler particles and/or reduce resin thickness [12-15], but all solutions have a slight reduction of vibration damping performance. Expulsion, which can be observed frequently during RSW, happens at either the faying surface or the electrode/work piece interfaces. The latter may severely affect surface quality and electrode life [16]. The risk of expulsion is especially high in spot welding of sandwich steel due to very dynamic and unstable character of the process, associated with melting and squeezing out the polymer core at contact area as reported by many researchers. Oberle and et. al. (1998) Optimized RSW parameters for VDSS to avoid expulsion by minimizing welding current-RMS during first welding cycle and using dome face electrodes [17]. The weldability of two variants (glued and brazed fibers) of thin sandwich stainless steel sheets with fibrous metallic cores was studied by Tan and et.al. (2007), both variants were found to be weldable and forming good quality weld nuggets with optimum welding parameters: electrode force 2.5 kN, weld current and weld time 4 kA, 200 ms, respectively [18].

Litecor<sup>®</sup> is a new sandwich lightweight sheet developed and invented by ThyssenKrupp Steel for automotive applications, which consists of two

thin outer layers and a core of polymer compound [19]. These new sandwich steel sheets are already used in inner parts; development target is outer panel parts. The development of new, sandwich steels for use in the automotive industry represents new challenges to the resistance welding of these steels as reported previously [20]. In this paper, a systematic study has been conducted on RSW of a novel sandwich steel (Litecor<sup>®</sup>) with two DP800 cover sheets, by applying an electrical shunt tool in order to melt and squeeze out the polymer from the welding zone to perform the welding. Numerical simulations with SORPAS<sup>®</sup> and many practical experiments were employed to evaluate the weldability of these materials.

## 2. Experimental Procedure

### Workpiece Materials, Electrodes and Welding Equipment

The experiments were conducted at the Technical University of Denmark (DTU). Workpiece materials were a sandwich steel and dual phase (DP800) sheets. The sandwich steel sheet is a newly invented lightweight material by ThyssenKrupp (German company producing many types of steels for automotive industries and others). The Litecor<sup>®</sup> (The commercial name of one type of sandwich steels) is produced with two thin outer layers of 0.2 mm steel sheets type BH200, and an interlayer of thermoplastic polymer compound 0.4 mm thickness, see Fig. 1.

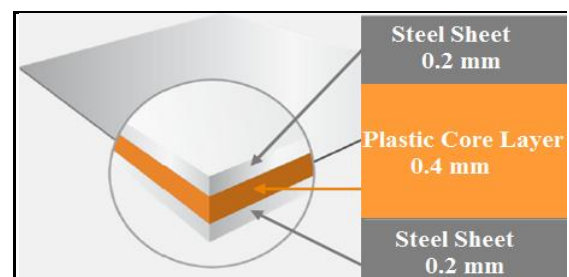


Fig. 1. The Litecor<sup>®</sup>; sandwich steel sheet [19].

Integrating the lightweight composite into the body-in-white is remarkably easy. It possesses the superior forming properties of conventional steel, with high flexural stiffness and buckling resistance; it combines high-level strength of steel with low weight of modern plastic. Moreover, it is suitable for paint-shop. Production starts with inner parts of vehicles and development target is outer panel quality, [21]. The density, tensile

strength, elongation, and hardness of the Litecor® which were tested at DTU are; 4.6 g/cm<sup>3</sup>, 200 MPa, 38%, and 80 HV, respectively, and the bending stiffness is 106% reference to steel. This composite material is very suitable to auto industrial. The cover sheets which were used to spot weld with sandwich sheet were hot-dip galvanized DP800 (DP stands for Dual Phase steel sheets consisting of a ferrite matrix and a hard second phase usually islands of martensite) steel sheets of 1.0 mm thickness, the properties and nominal compositions are shown in Table 1.

The delivered sheets were cut into 105 × 45 mm, with longitudinal dimension in the rolling direction. They were welded as a lap joint ready for subsequent tensile-shearing testing as shown in Fig. 2 according to the International Standard ISO 14273 [22]. Tensile-shear testing was carried out using AMSLER a universal testing machine at a deformation rate of 2 mm/min to determine the weld strength.

A hard wood fixture was used to mount the samples in good alignment with the electrodes. A shunt tool was designed and made from pure copper, which was used in all practical experiments for conducting current in 1<sup>st</sup> pulse. The electrode tips (Female Cap) were of type B0 according to ISO 5821-2009 and the American standard RWMA No. FF-25, [23]. They were made of zirconium-copper alloy (CuCrZr) with the following chemical composition; Cr: 0.7-

1.2%, Zr: 0.06-0.15%, bal. Cu. The electrodes were of truncated configuration, Ø16 mm in diameter with a flat tip surface of 6 mm, [24].

RSW experiments were performed on a TECNA 8105 AC welding machine with weld controller of type TE-180; specifications of the machine are listed in Table 2. The welding current was measured by a Rogowski coil together with a precalibrated TECNA-1430 conditioner, and a Kistler piezoelectric force transducer was used to measure the electrode load. The acquired data (DAQ) were treated on a PC by specially developed software in LabVIEW, see Fig. 3.

The following parameters of the RSW process were calculated for each experiment, current RMS I (A), welding time C (s), and the electrode force P (kN). Tensile-shearing tests were carried out using a universal testing machine at a deformation rate of 2 mm/min to determine the weld strength S (N). Vickers microhardness measurements were performed using sophisticated instrument (FUTURE-TECH, FM-700) with load of 100-g testing on weld cross-sections in longitudinal direction through the diameter of the nugget at intervals of 0.5-1.0 mm. Macrographs and micrographs of the welds were made in light optical microscope (LOM) type Nikon ME600. Moreover, high-resolution images were made in SEM, JEOL JSM-5900 with LaB6 filament applying secondary electron (SE) at 20 kV, and using EDS for quantitative chemical analysis.

**Table 1,**  
**Mechanical properties and nominal composition of DP800 cover sheets [25].**

Yield Strength (MPa)	Tensile Strength (MPa)	Elongation	Hardness (HV)	Chemical composition (wt-%)							Coating (Zn) Thickness
				C	Si	Mn	Cr	Al	P	S	
500-640	800-950	12%	200	0.16	0.25	1.9	0.5	.015	.02	.004	7 μm

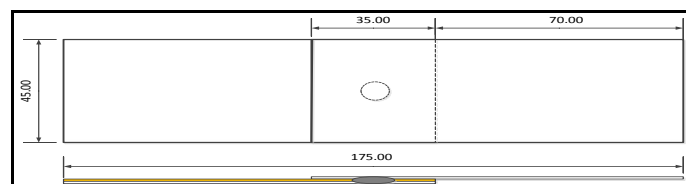


**Fig. 2. Schematic illustration of lap joint for tensile-shearing testing.**

**Table 2,**  
**Machine specifications and image, TECNA AC welder.**

Specifications	Values	Specifications	Values
Controller	TE-180, 16 Functions	Nominal power at 50%	250 kVA
Supply Voltage	380 V	Phases	1
Frequency	50 Hz	Supply pressure	6.5 bar
Max. welding current	68 kA	Electrode force per 1 bar	3.14 kN
Max. welding force	18.85 kN	Throat depth	250 mm
Max. welding Power	810 kVA	Water cooling	12 ℓ / min

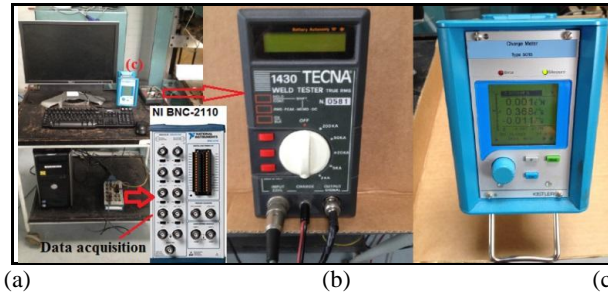
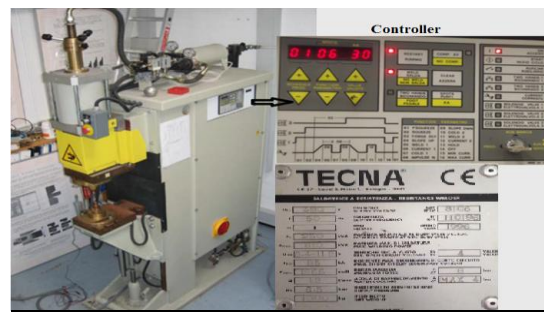


Fig. 3. Instruments images, (a) Computer used to collect all the measurements with (DAQ), (b) Weld tester connected to Rogowski coil, (c) transducer connected to load cell.

### Welding of Sandwich Steel

The sandwich steel (Litecor<sup>®</sup>) has a polymer core between two steel sheets and it is required to weld with two other cover steel sheets. The polymer core does not conduct electricity; therefore current will not pass through proposed area and definitely there is no creation of nugget (welding area). Preliminary studies by ThyssenKrupp Steel have proved that the lightweight sandwich steels can be resistance spot welded to other steel sheets with a special setup of shunt connection.

The Litecor<sup>®</sup> was already used in the inner panel of some vehicles, and the goal is to use this material in the outer panel especially for light weight vehicle as electrical cars [26]. Therefore, it is required for outer panel to weld the sandwich steel with other sheets in three combinations as shown in Fig. 4; (1) with upper and lower cover sheets, which was used in this work, (2) with one cover sheet only, and (3) with two cover sheets in one side, as recommended by automaker. There are two challenges related with resistance spot welding of sandwich steel with cover sheets for inner panels including; non electrical conductivity of the polymer core and the severe expulsion of the polymer due to rapid melting and squeeze out of the polymer in the first stage of welding operation, which affects the quality of welding. While for the outer panels, there is a third challenge in addition of the two aforementioned challenges; it is not good appearance of the welding area due to the high indentation.

However, a shunt tool was designed and made from pure copper to perform the resistance welding of sandwich steel with DP800 cover sheets to resolve a non-conductivity problem of a polymer core.

Fig. 5 illustrates the idea of using the shunt tool. The welding of sandwich steel with non-conductive electrical polymer core required two steps; the current passes through the shunt tool at first step, as shown in Fig. 5-a, which needs the shunt tool to be close as much as possible from the electrode (proposed welding area), thus a high current will pass through metal sheets and will heat them, therefore the polymer core at this area will melt and squeeze out by electrodes pressure. Once all four metal sheets have been contacted in this region the second step starts; the current will flow directly in the welding area and the generated heat will melt the metal in this region formation the nugget, see Fig. 5-b. For this reason, in the 2<sup>nd</sup> step needs the shunt tool to be far as much as possible from the electrode, because if not some of the current will pass through the shunt tool and will lose part of energy, and will adversely affect quality of the welding. Thus, it is required to be accurate where selecting the distance between the electrode and the shunt tool due to the inversely relation of this selection of distance between the 1<sup>st</sup> and 2<sup>nd</sup> steps. Thus, all simulations and practical experiments in this work were done with two pulses and some of them with three pulses.

Much effort has been devoted to find the optimum distance between the shunt tool and the

welding area by carrying out many numerical simulations and practical experiments. Three different width of wood fixture were used related with this distance to find the optimum value, see Fig. 6. But the results were discussed later are only with distance of 19 mm, which is used in this work. Because of the lack of information on welding a new sandwich steel material, it was very difficult to find the optimum welding parameters. Therefore, in the beginning of this work many simulations and optimizations with SORPAS<sup>®</sup> 2-D were carried out with different set up of welding current, welding time, electrode force, and multi pulses.

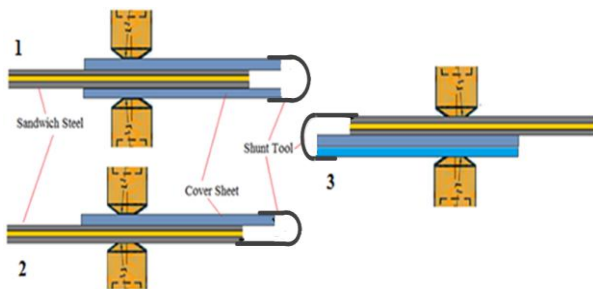


Fig. 4. Three possible combinations for welding the sandwich steel with cover sheets

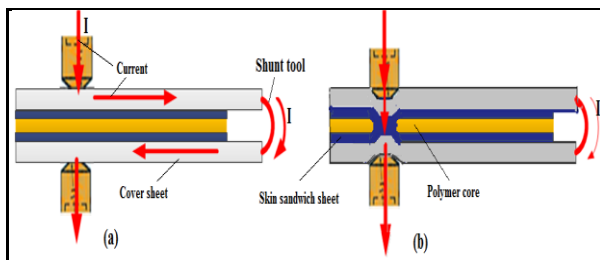


Fig. 5. (a) Current flow through shunt tool 1<sup>st</sup> step, (b) current pass through welding area 2<sup>nd</sup> step.

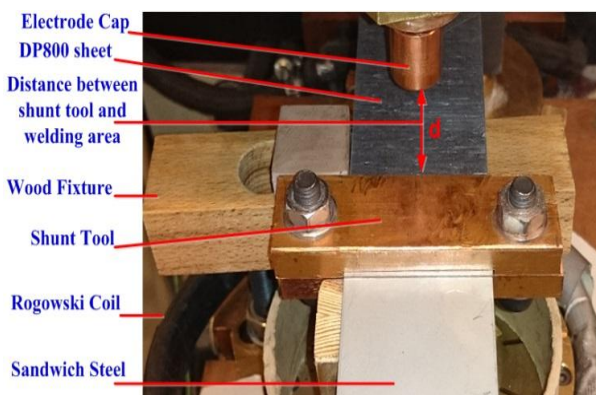


Fig. 6. Set-up for welding (left), Three different thicknesses of hardwood-fixtures related with (d) (right).

### 3. Results and Discussion

#### Numerical Simulations with SORPAS<sup>®</sup> 2-D

Commercial finite element numerical program SORPAS<sup>®</sup> from SWANTEC [27] was used in this work. It is well known and most widely used as a numerical tool for simulation, optimization, and planning features of the resistance welding processes. It is based on mechanical, electrical, thermal, and metallurgical models. The resistance spot welding process of sandwich steel with other cover sheets is a 3-D case. However, this can be carried out with 2-D numerical simulation at first glance to get preliminary information about the welding parameters of resistance welding of Litecor<sup>®</sup> with cover sheets of DP800.

Due to the fact that Litecor<sup>®</sup> is a new sandwich steel material, therefore there is not much knowledge about the welding parameters and the conditions necessary to simulate the weld process with it. In order to carry out the simulations of the process, a special material data were prepared by SWANTEC and implemented for the polymer core in the material database as with and without transformation, i.e. in case of 1<sup>st</sup> step when the polymer in its location before heating and melting, and 2<sup>nd</sup> step after squeeze out the polymer from the welding area. This treating of the polymer core in simulations is shown in the Fig. 7. Moreover, a third tool was added in setup of input data of simulation as a shunt tool for conducting electrical current between the cover sheets through the shunt connection, as shown in Fig. 8, which illustrates in the bottom of the figure. The setup input values of this simulation include; 3.5 kN, (10 kA, 4 cycles), (14 kA, 4 cycles), and (14 kA, 4 cycles) electrode force, welding current and welding time for the three pulses respectively. When the sheets are heated up, the polymer core in the sandwich steel will be

melted and the outer sheets of the sandwich steel will be pressed into contact under the weld force. Therefore, the resistance spot welding process will be realized when the steel sheets get into contact.

Fig. 9 shows the result of a previous setup simulation, Fig. 9-a & b indicate the current flow as a current density ( $A/mm^2$ ) before and after the polymer squeeze out, i.e. the current flow through the shunt tool and through the welding area respectively. While Fig. 9-c indicates the temperature distribution in the sheets and the electrodes, as the same time it shows the heating and breaking of the polymer core, which is low melting temperature. Fig. 9-d illustrates the final stage of the process and the nugget formation with splash arrow indicates the location of extrusion of the molten metal. The splash was occurred due to the high current set up input (14 kA) in the 2<sup>nd</sup> and 3<sup>rd</sup> pulses, which were more than the required current to form the nugget.

More than 70 simulations were performed by changing the welding parameters input; welding current and time, and electrode force. Some simulations were performed with 3 pulses instead of 2 pulses with slope of current in 1<sup>st</sup> pulse to find the optimum of these values and the weldability of the Litecor<sup>®</sup>. Fig. 10 shows the relation between the nugget size as an average diameter of the welding area and the heat input (J). This relationship is very normal because increasing the amount of electrical energy input will lead to increasing the amount of heat generated and thus an increase in the amount of molten metal forming a large welding area (nugget).

Table 3 shows the result some of selected simulations, which is ordered as maximum value of ratio of the nugget average diameter to the heat input (last column), Which is always preferred to consume less energy and get the largest size of the nugget as stated in the RWMA [9]. Noteworthy, the values of the heat in the 3<sup>rd</sup> column of this table were calculated already by the SORPAS. While the average diameter of the nugget, which refer to the weld size (2<sup>nd</sup> column) was calculated as the average of the two diameters (large and small diameter) of the oval (the normal shape of the nugget) were calculated by the program. The column of nugget/time in this table indicates the ratio of the nugget average diameter to the total process welding time, which is also preferred due to the fact that resistance spot welding designed as a very fast process and this is required especially in the auto manufacturing. The column of the slope 1<sup>st</sup> pulse demonstrates if there is slope in

this pulse or not, and the slope time, which is one cycle in many instances.

After analyzing these simulations, it was concluded that the 1<sup>st</sup> pulse should have a lower current than the 2<sup>nd</sup> pulse due to the fact that first pulse function is only for heating and melting the polymer core, and the function of the second pulse is to form the welding by melting the four contact metal sheets in this region. The use of a third pulse did not improve much the quality of welding and so on for using slope in the first pulse. Therefore, these functions were not used in the practical experiments. The results of these simulations were recommended that the optimum electrode force is 3.5 kN and this value was used for the most practical experiments and the simulations with SORPAS<sup>®</sup>3-D.

Fig. 11 demonstrates the report of simulation No. (70), which is considered a good setup input, which led to a minimum splash and sufficient weld size. However, the gap between the current in the 1<sup>st</sup> and the 2<sup>nd</sup> pulse is equal to ( $9.5 - 5.5 = 4$  kA), which is considered a large value and will adversely affect the welding machine and the lack of stability during welding process, and hence on the quality of the welding, as well as the risk that may be caused to workers. Consequently, the numerical simulations greatly assisted while doing practical experiments through non exposure to the significantly problems, especially in the subject of the last conclusion. In the left bottom of the figure shows the weld growth curve. The nugget was start forming after 190 ms in the 2<sup>nd</sup> pulse and continue growth until reach the maximum nugget size that is 4.539 mm, which is the upper limit of these input set up parameters values even if the welding continued up as a welding time increase, but the contrary, in the case of increasing the welding time adversely affect the welding quality due to increasing the expulsion of the molten metal.

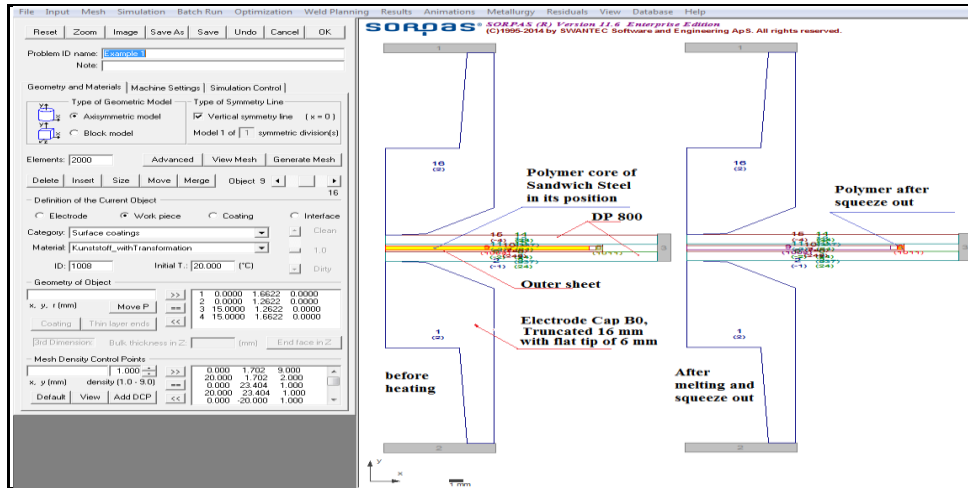


Fig. 7. Set up of the input material data of simulation with SORPAS® 2-D.

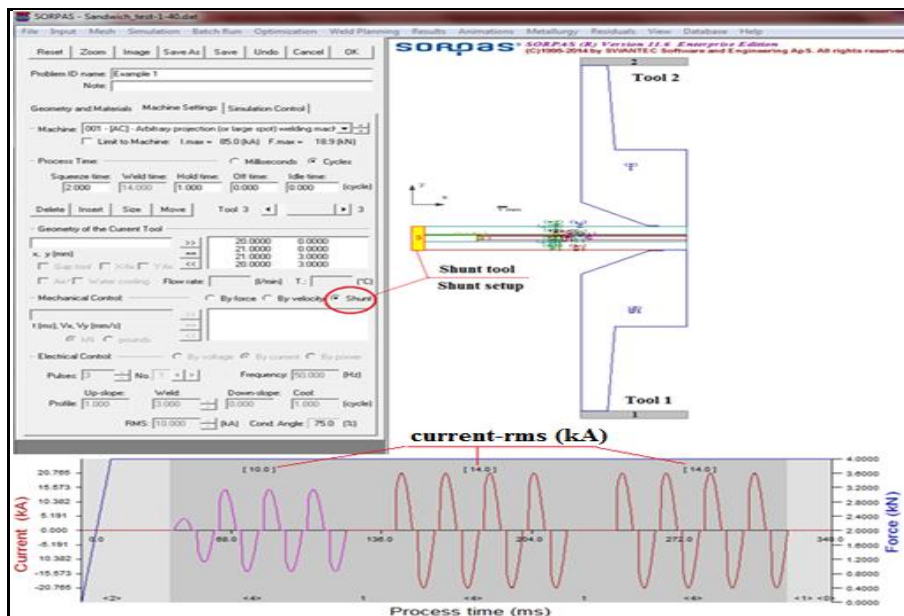


Fig. 8. Set up of the adding third tool as a shunt in simulation with SORPAS® 2-D.

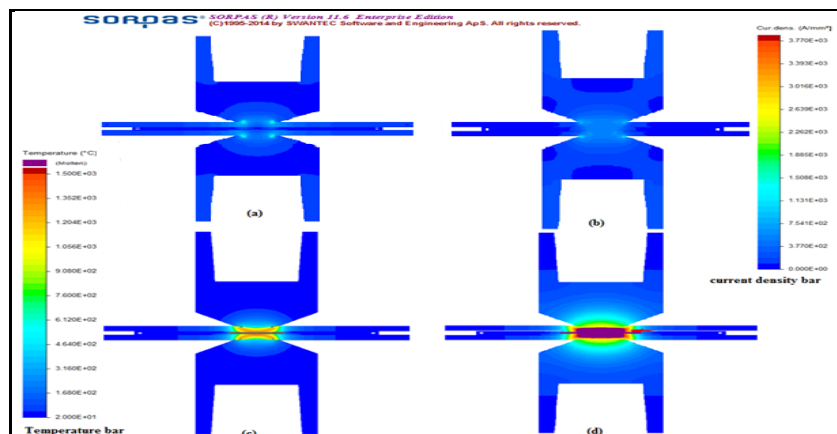


Fig. 9. Simulation results of spot welding of Litecor® with two cover sheets DP 800, (a) Current flow in cover sheets through shunt tool, (b) Current flow through welding area. (c) Heating and breaking of polymer core, (d) Nugget formation at the final process with splash arrow.

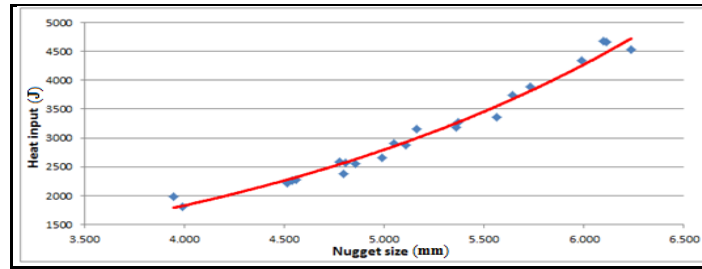


Fig.10. Relationship between the heat input and the nugget size

Table 3, Results of some selected 2-D simulations

Ex. No.	Nugget dia. avg.	Heat (J)	Total times cycles	Current Type: AC						slope 1st. Pulse	Force kN	Nugget/ time	Nugget/ Heat
				Pulse 1		Pulse 2		Pulse 3					
				I (kA)	cycles	I (kA)	cycles	I (kA)	cycles				
73	3.992	1813	12	5.1	7	8.52	5			No	3.5	3.327	2.202
54	4.516	2215	12	5.87	7	9.58	5			No	3.5	3.763	2.039
37	4.795	2385	8	8	4	12	4			3+1	3.5	5.994	2.010
70	4.539	2265	12	5.57	6	9.47	6			No	3.5	3.783	2.004
74	4.557	2277	13	5.87	8	9.58	5			No	3.5	3.505	2.001
50	3.947	1992	13	6	8	8	5			No	3.5	3.036	1.981
38	4.854	2561	8	8	3	12	5			2+1	3.5	6.068	1.895
62	4.988	2659	10	7.3	5	11.54	5			4+1	3.5	4.988	1.876
72	4.808	2570	12	6.9	7	10.18	5			No	3.5	4.007	1.871
59	4.777	2581	13	6.85	8	9.79	5			No	3.5	3.675	1.851
71	4.777	2581	13	6.85	8	9.79	5			No	3.5	3.675	1.851
55	5.108	2884	10	8.01	4	11.55	6			3+1	3.5	5.108	1.771
61	5.047	2904	8	9.96	3	12.58	5			2+1	3.5	6.309	1.738
66	5.359	3182	12	6.89	6	12.03	6			No	3.5	4.466	1.684
64	5.562	3366	9	7.67	4	14.31	5			No	3.5	6.180	1.652
43	5.369	3271	8	10	3	14	5			2+1	3.5	6.711	1.641
56	5.161	3149	10	9.23	4	11.75	6			3+1	3.5	5.161	1.639
60	5.643	3735	10	9.24	4	13.74	6			3+1	3.5	5.643	1.511
44	5.731	3893	10	10	4	14	6			3+1	3.5	5.731	1.472
65	5.989	4344	10	10.57	5	14.95	5			No	3.5	5.989	1.379
40	6.238	4527	12	10	4	14	4	14	4	3+1	4.0	5.198	1.378
39	6.112	4668	12	10	4	14	4	14	4	3+1	3.5	5.093	1.309
58	6.100	4682	16	9.43	8	12.29	8			7+1	3.5	3.813	1.303

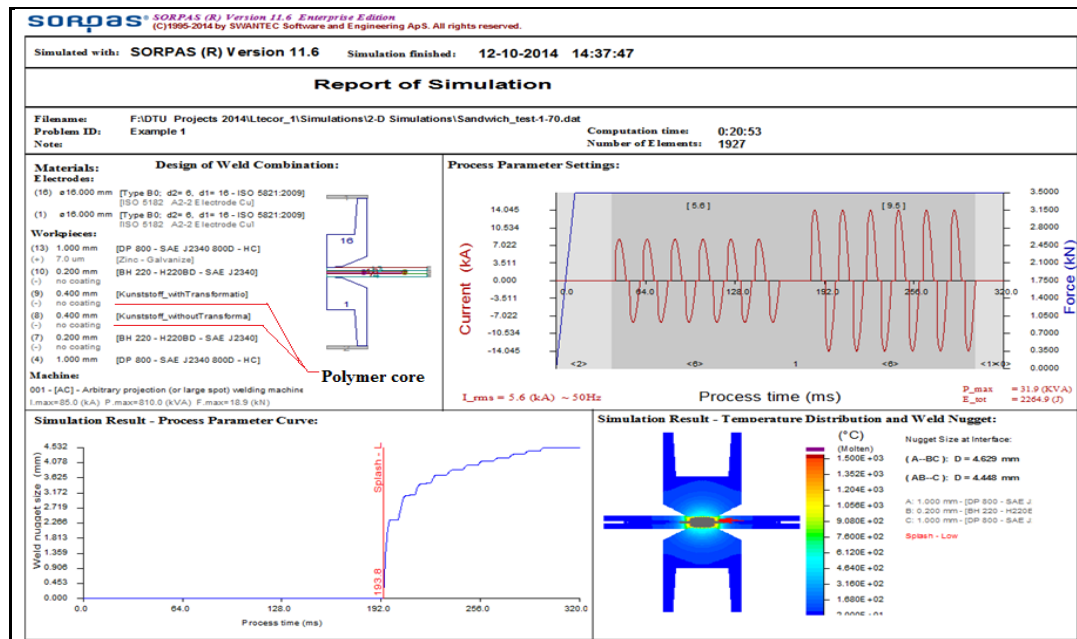


Fig. 11. Report of simulation No. 70.

## Weldability of Litecor<sup>®</sup>

The optimum welding parameters values were found from the numerical simulations, which were the only information available due to the recent development of the Litecor<sup>®</sup>. These simulations provided knowledge of the possible ranges of current, time, and force that were used later in the practical experiments to examine the weldability of the Litecor<sup>®</sup> with cover sheets of DP 800. It is worthy to point out that more than 50 welding processes were done and calculated the welding parameters by LabVIEW and excel sheet, then the welding specimens were examined for strength and macro/micrograph. The aim of all these experiments was to find the weldability of the Litecor<sup>®</sup> with DP800 cover sheets; weldability means the range of values from the minimum to the maximum of the welding current, welding time, and electrode force, i.e. the safety zone of the welding parameters and forming sound welding (good quality welding without defects).

Table 4 demonstrates some of selected experiments ordered as the ratio of the failure force in (N) to the current difference (gap). There are many details were mentioned in the table, the first fourth columns are the values set up input welding machine functions, followed by columns including the calculated values of the electrode force (kN) and current as RMS (kA). Moreover, a difference values between the current flowing through the shunt tool before melting the polymer core and the current flowing through welding area after squeeze out the polymer are included. This gap is very crucial especially with high values, which negatively influences the stability of the machine and welding quality, as well as the risk that workers may be exposed such as the splash of molten metal. The strength of the weldments and the mode of failure are included, which were tested in the lab by using a tensile-shearing test

and the mode of failures were examined visually. The interfacial failure predominantly occurs with lower strength of the welding attributed to the smaller size of the nugget, and vice versa where plug (button) failure occurs with higher strength and larger nugget size, and this is in line with other researchers (Ma and et. al) [28], Pouranvari [29] and others.

The welding time and the most of welding current setup in the 2<sup>nd</sup> pulse were fixed at 5 cycles and 10 kA to analyze the welding process with different setup input of 1<sup>st</sup> pulse, which is considered as a function of breaking and melting the polymer core. Increasing the welding current input in 1<sup>st</sup> pulse (20 kA) did not give good welding process due to the large gap (6.64 kA). In contrast, decreasing the welding current in the 1<sup>st</sup> pulse gave a good welding. This is well illustrated in the Fig. 12, a large gap (current before and after melt and squeeze out the polymer) means unstable process; (14.31-7.67=6.64 kA) as Ex. No. (12), and a small gap means stable process; (8.37-5.50=2.87 kA) as Ex. No. (16), this is well illustrated in the curve of electrode force.

The set up input of the welding current in 1<sup>st</sup> pulse preferably to be as lower value as possible with long time in order gap be a minimum value, however, a very low current input setup as (1 kA in Ex. No. (35)) did not give a sufficient nugget size and good strength due to the delay of melting and squeezing out of the polymer, which occurs in 2<sup>nd</sup> pulse not in the 1<sup>st</sup> pulse as usual. Although, an extreme increase in the amount of welding current in the first and second pulse as Ex. No. (8), (11), (12), and (20), did not observe a significant increase in the welding strength, it believes the reason is that there is a large gap (current welding difference before and after melting the polymer). In conclusion, the Ex. No. (32) is considered a good welding set up input, which gave a lower gap (2.22 kA) and high strength (12887 N).

**Table 4,**  
Results of some selected Practical experiments.

Ex. No.	Machine setting functions input				calculated values					rising time (ms)	current difference before and after rising	Failure Force (N)	Ratio failure force to current difference	Failure Mode	Nugget Size (mm)
	1st. Pulse		2nd. Pulse		Force (kN)	current rms (kA)									
	5 cycles welding time	6 kA welding current	11 cycles welding time	12 kA welding current		1st. Pulse	2nd. Pulse	before rising	after rising						
32	9	4	5	10	3.52	5.23	9.33	4.38	6.60	120	2.22	12887	5805	Plug	3.30
27	9	7	5	10	3.50	5.81	9.54	5.00	8.02	140	3.02	14210	4705	Plug	3.40
26	8	7	5	10	3.48	5.20	9.35	4.74	7.64	140	2.90	12985	4478	Plug	3.35
30	8	6	5	10	3.49	5.37	9.58	4.72	7.55	130	2.83	12495	4415	Plug	3.50
33	9	3	5	10	3.51	4.44	9.30	4.03	6.09	150	2.06	9016	4377	Int.	3.10
29	6	9	5	10	3.48	5.77	9.31	5.46	8.40	100	2.94	12397	4217	Plug	3.65
22	8	8	5	10	3.42	5.87	9.58	5.39	8.48	140	3.09	12985	4202	Plug	5.15
16	7	10	5	10	3.47	6.07	9.66	5.50	8.37	120	2.87	12054	4200	Plug	3.62
34	9	2	5	10	3.56	4.13	9.14	3.85	5.88	160	2.03	8428	4152	Int.	3.20
19	8	10	5	10	3.48	6.98	9.82	5.97	9.38	120	3.41	13400	3930	Plug	5.20
24	7	9	5	10	3.50	5.75	9.56	5.19	8.31	120	3.12	12114	3883	Plug	4.40
23	8	9	5	10	3.51	6.36	9.74	5.31	8.79	120	3.48	12838	3689	Plug	4.70
39	7	8	5	10	3.50	6.08	9.56	5.28	8.36	110	3.08	10633	3452	Plug	3.45
8	3	25	6	15	3.48	9.24	13.74	9.24	13.74	80	4.50	14996	3332	Plug	4.73
20	7	12	5	10	3.44	6.90	10.18	6.18	10.18	120	4.00	12936	3234	Plug	5.20
28	6	8	5	10	3.50	5.15	9.38	5.15	9.38	120	4.23	11760	2780	Plug	3.80
31	8	5	5	10	3.48	4.59	9.25	4.59	9.25	160	4.66	12838	2755	Plug	3.65
11	6	20	5	15	3.51	10.99	12.35	7.29	13.54	60	6.25	15425	2468	Plug	5.80
12	4	20	5	20	3.31	7.67	14.31	7.67	14.31	80	6.64	15092	2273	Plug	6.00
35	9	1	5	10	3.64	3.69	8.86	6.06	9.12	210	3.06	5880	1922	Int.	3.00

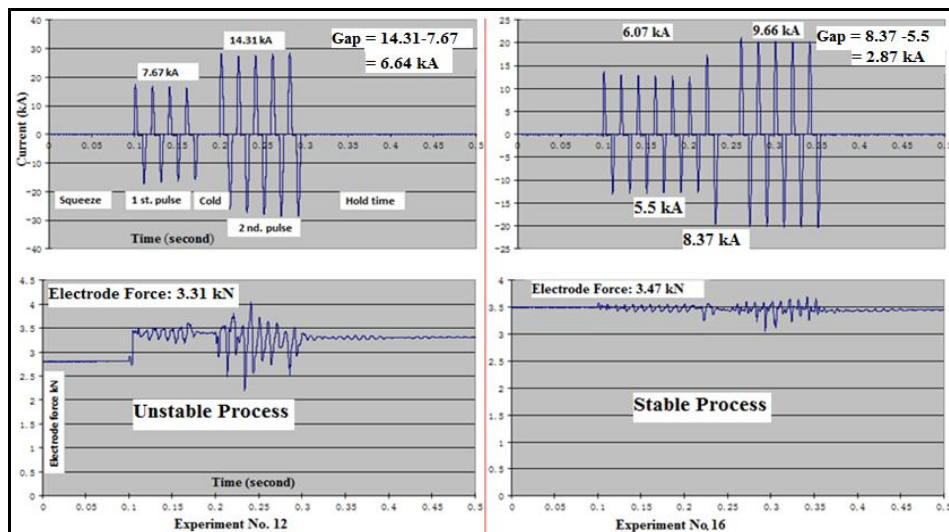


**Fig. 12** Comparison between two experiments, (left) instability process (large gap), (right) good welding process (small gap).

**Microhardness Test**

A hardness characteristic of the resistance spot welds is one of the most significant factors influencing their strength and failure mode. The images of macrostructures including microhardness test points and their values for Ex. No. (8), (12), (16), and (23) is shown in the Fig. 13-a, b, c, d respectively. These specimens are selected for the different nugget sizes due to the

different related welding parameters as shown in the previous table. The substantial difference in the composition of the constituent materials for spot welds led to a significant difference in microhardness from point to point. However, all points in the weld zone and in the HAZ exhibited a significant hardness increase from the base metals (BH200 & DP800), due to the high content of alloying elements in these steels as well as the high cooling rate. This conclusion is expected and

well-known from other researchers such as (Ma and et. al. 2008). However, a very wide variation of hardness even within the weld area due to the Litecor® consisting of several layers and spot welded with two DP800 steel sheets. It is worthy to point out that the values of the hardness of the base metals for BH200 and DP800 are about 80 and 208 HV sheets respectively.

Fig.14 illustrates the profiles of the microhardness for the four specimens (8, 12, 16, and 23). All these specimens show highest magnitudes of hardness in the middle of the weld zone and start to fall towards the outskirts of the nugget due to the difference in the size of the crystal structure as a result of the different cooling rate from one region to another, whenever smaller crystal higher hardness. While the HAZ has also gained a very high hardness and this is clear in

inflexion of the curves due to apparently attributed to the formation much of martensite result of the highest cooling rate in this region, which is the closest to the cold base metal. The difference in hardness curves arising from variation of the welding process parameters, where notice that the highest curve represents the hardest weld, which is the specimen No. 12 due to greater amount of heat input led to the formation of relatively large size of the nugget, and this is clear from the length of the curve compared to the other curves. The hardness curve of the specimen No. 16 is the lowest than the rest, which is smallest nugget size due to the lack of the amount of heat input during the welding process. While, the hardness curves of the two other specimens are located between the highest and lowest curves.

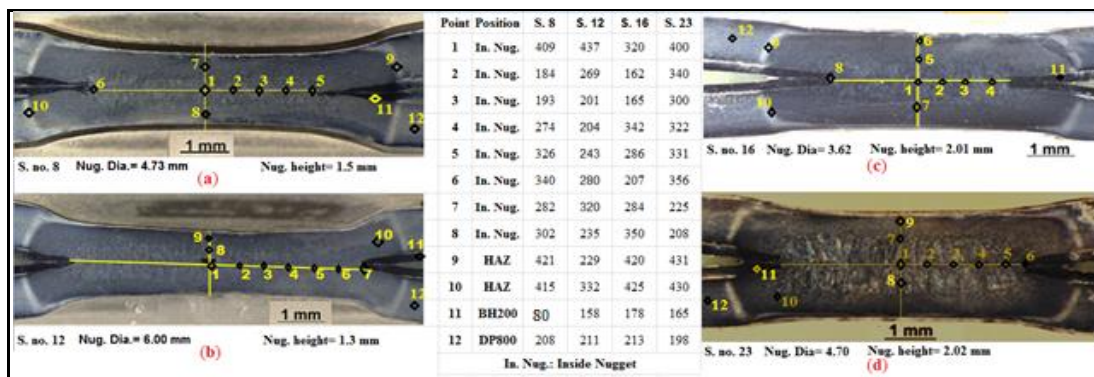


Figure 13 Images of macrostructures including microhardness test points with table of their values.

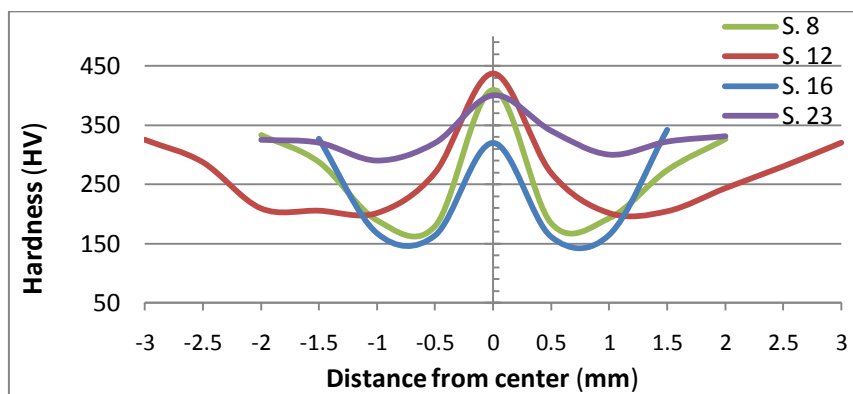


Fig. 14. Microhardness curves.

### Macro/Micrograph Examinations

Dual phase steels typically consist two phases including; body centered cubic (BCC)  $\alpha$  –ferrite and a dispersed body centered tetragonal (BCT) hard martensite in the form of islands, usually they are low-carbon low-alloy materials with 10-40% martensite embedded in a ductile ferrite

matrix [30]. There were a significant changes in the microstructures after spot welding the cover sheet DP800 with sandwich steel Litecor®, since these materials are transformable.

Light optical microscope was used to examine the microstructural variations as shown in Fig. 15, which illustrates the macro/microstructures of the specimen No. 8 after spot welding. Fig.15-a

shows the macrograph of cross section of the weld area indicates all distinct regions including the base metals, HAZ, and the nugget with its diameter. The microstructure of the base metal of DP800 consists of eventually distributed martensite (white phase) within the ferrite phase (dark phase). Martensite becomes larger and its volume fraction is higher in the HAZ than in the base metal as shown in outskirts of Fig.15-b. If there is no other type of steel such as BH200 (outer layer of Litecor<sup>®</sup>) in the center of the fusion zone was all that area full with martensite. The presence of this thin layer of steel with low carbon reduced the presence of the hard martensite, as shown in Fig. 15-c, d, and e. However, this region showed hardness higher than the base metal as previously mentioned.

To understand the variation in microstructure in resistance spot welds, the welding process parameters (electrode force, weld current, and weld time) are considered as a heat input. While the cooling rate depends on hold time and other factors, which is very high in this case, also needs to be considered.

In this specimen (No. 8) no voids could be observed within the nugget. However, there is a deep penetration of electrodes toward the cross section of the sheets due to the high current passing through the welding area (9.23, and 11.75 kA RMS for 1<sup>st</sup> and 2<sup>nd</sup> pulse respectively), and cause surface crack as shown in the Fig. 15-f. For

the same former reason, a large separation between welded sheets in the case of high welding current and electrode force setup input as shown in Fig. 16, which represent the specimen No. 12. This specimen has a large nugget diameter (6.0 mm) due to higher welding RMS current in 1<sup>st</sup> and 2<sup>nd</sup> pulses (7.67 and 14.31 kA) respectively. Although this specimen has a large nugget size but the high welding current in the 2<sup>nd</sup> pulse affects negatively in the welding quality, which represents by presence of very large void and cracks as shown in Fig. 17.

Fig.18. demonstrates the comparison between specimen No. 16 and specimen No. 23 in the nugget size. The nugget diameter of specimen No. 16 is smaller than specimen No. 23 in spite of the current setup input in 1<sup>st</sup>. pulse is higher (10 kA for S. 16 and 9 kA for S. 23), see table 4. It is therefore concluded that it is preferred to input set up a lower current and relatively long welding time in the 1<sup>st</sup> pulse, for forming a good weld without defects and a suitable nugget size thus a sufficient strength. It is believed that the lower current input and longer welding time in 1st pulse; allow heating the sheets to a required temperature for melting the polymer core in the welding area without much penetration of electrodes into the sheets and not generate considerable heat, which leads to occurrence of the expulsion and the sheets separation.

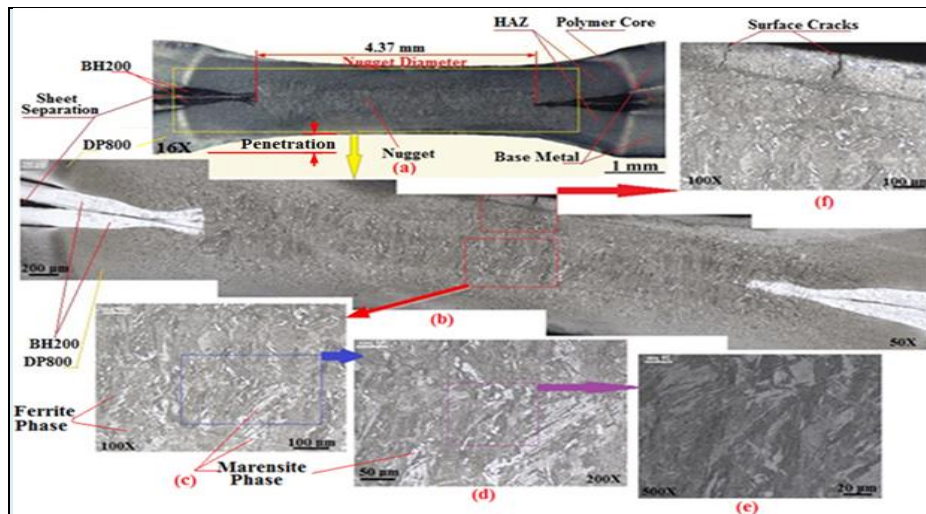


Fig. 15. Macro/Microstructure images of specimen No. 8.

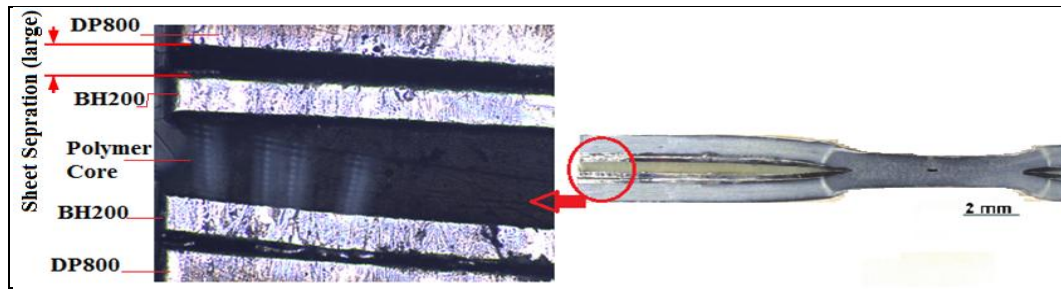


Fig. 16. Macrograph of specimen No. 12 indicating large sheets separation.

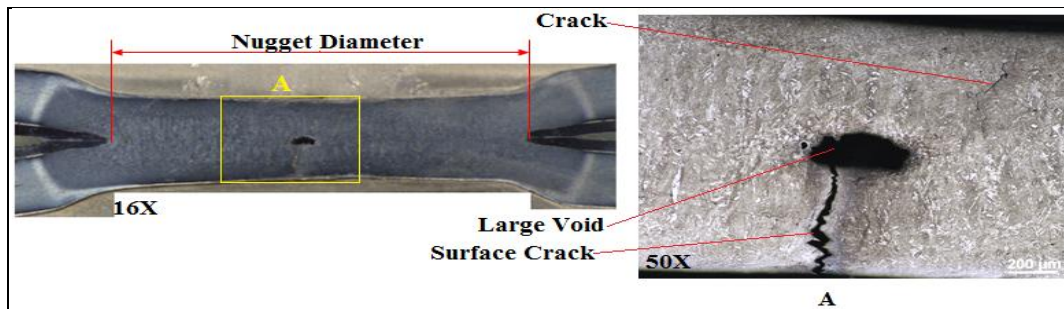


Fig. 17. Macro/Microstructure images of specimen No. 12.

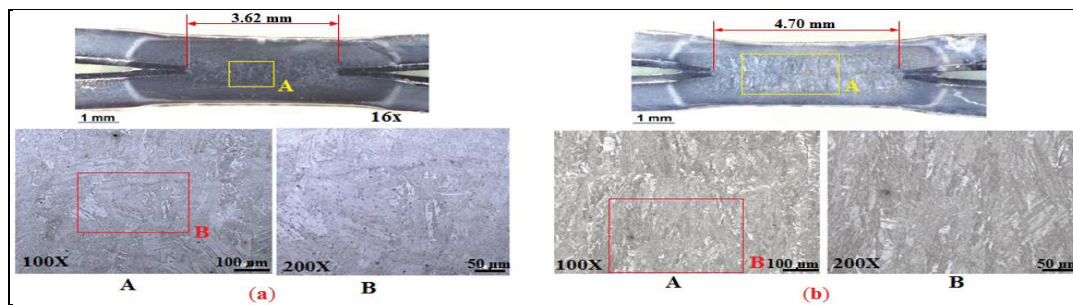


Fig. 18. Macro/Microstructure images of specimen No. 16 (a), specimen No. 23 (b).

### SEM/EDS Examinations

Micrographs were also made in SEM to study microstructure and carry out high-resolution mapping determining chemical composition of areas of special interest by X-ray spectroscopy (EDS). Fig. 19 shows the microstructures of the welding area for specimen No. 8 and 23. There is no large variation in the microstructures between them due to the amount of heat input during the welding process almost equal, creating the same welding area and very close in size. High content of martensite is observed a result of the transformation because the metals contain a high percentage of carbon and manganese as well as the higher cooling rate because of the mechanism of the RSW process that focus the heat to a small area and in the contrast the adjacent areas will be cool. There is insufficient time for carbon diffusion at such high cooling rats. Moreover, both the higher carbon and manganese contents in

DP800 also result in a higher hardenability. No voids could be observed in these areas due to the welding parameters were below the case of expulsion.

Fig. 20 indicates the spectrum analysis of the welding area of specimen No. 8, significant variations in the proportions of the elements from one region to another, which is seen in image. The proportion of these elements are very close to what previously reported in table 1 that was adopted by the metal sheet supplier. The presence of metallic elements chromium and manganese being alloying elements in DP800, while having a little proportion of zinc metal is because of that sheet is coated with this metal. In the other hand, Fig. 21 shows the spectrum analysis of surface of DP800 sheet, which is coated with zinc that is recorded in high proportion value (95.4%). While having a small presence of oxygen is believed due to the preparatory processes prior to implementation of SEM tests.

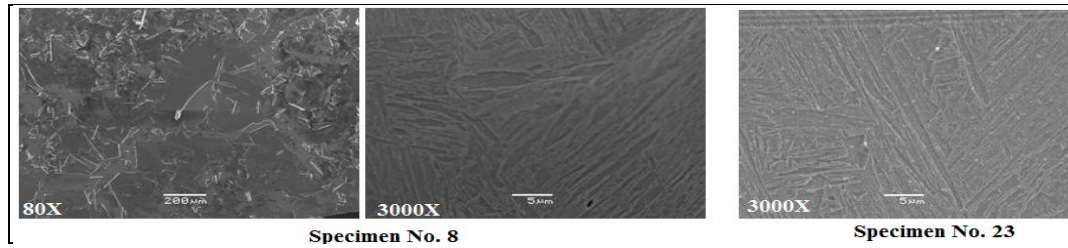


Fig. 19. SEM images for specimen No. 8 and 23.

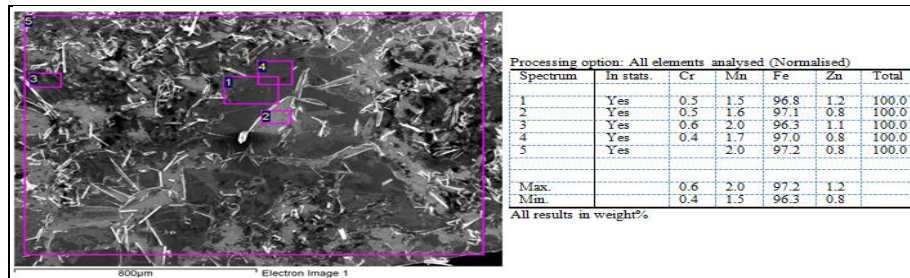


Fig. 20. Spectrum analysis of specimen No. 8.

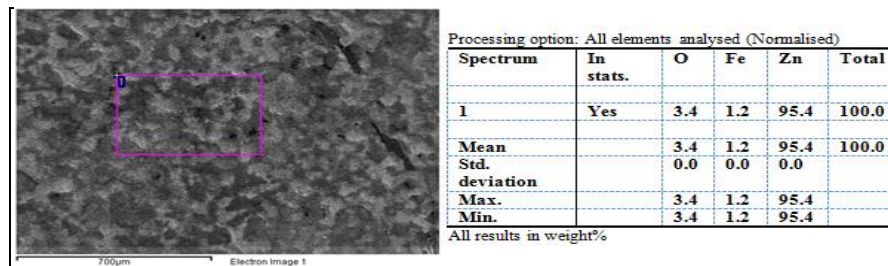


Fig. 21. Spectrum analysis of surface of DP80 sheet coated with zinc.

### Tensile-Shearing Tests

Tensile-shearing tests of the welded joints indicate their strength and the failure mode. Fig. 22 shows the maximum fracture load for the spot welds as a function of the welding energy input specified in table 4. The energy input (heat) is calculated based on current squared multiplied in welding time for 1<sup>st</sup> pulse plus 2<sup>nd</sup> pulse, while other parameters are kept constant such as electrode force. Therefore, it could be considered that electrical resistance value had been fixed for all practical experiments. The data point, which was represented in the figure, is the average of three specimens test.

The mode of failure was recorded in each test and classified as one of the following three types: (1) interfacial failure (nugget fracture in shear), (2) plug failure (nugget pull-out), and (3) failure in the heat affected zone (HAZ). Failure mode (1) typically occurs at low energy input indicating insufficient heating, in this case is about (600

ka<sup>2</sup>×second). And mode (2) at sufficient energy input, which is a higher than 600 and lower than (1600 ka<sup>2</sup>×second) indicating satisfactory heating. While mode (3) at a higher energy input, this is more than the last value indicating overheating and softening of the region near the nugget. It is seen in general that with increasing energy input the maximum load sustained by the spot-welded joints increases. The fracture load was seen to reach the maximum value in the range of energy input (1400 to 1600 ka<sup>2</sup>×second). Beyond this energy range corresponding to the expulsion, in line with other researchers Senkara et al., 2004 [16]; Pouranvari and Ranjbarnoodeh, 2011 [31], and others, high heat input welding conditions lead to increasing the probability of expulsion occurrence as well as its extent and its associated electrode indentation. The electrode indentation induced surface cracks beyond the expulsion energy input, as shown in figure 17.

The second impulse current condition was strongly influenced on the failure mode of

sandwich steel with cover sheets DP800, which in fact is associated with the microstructural changes occurring in the weld nugget. High current input setup in the 2<sup>nd</sup> pulse will increase the electrode indentation, thus will not give good appearance, which is required especially with outer panel. Because of high current setup input (20 kA) such as Ex. No. 5 and 12 gave a deeply indentation as shown in Fig. 23. And the same thing will be occur if the weld time is increased, heat conduction into the surrounding metals becomes greater, causing greater warpage, sheet separation, and deep indentation.

In summary, mode (2) in failure exhibits strong welding and it is related with sufficient nugget size. Therefore, the suitable range of the energy input is between 800 to 1600 kA<sup>2</sup>× second, and this is corresponding to (5-6) cycles and (10-15) kA for welding time and current respectively.

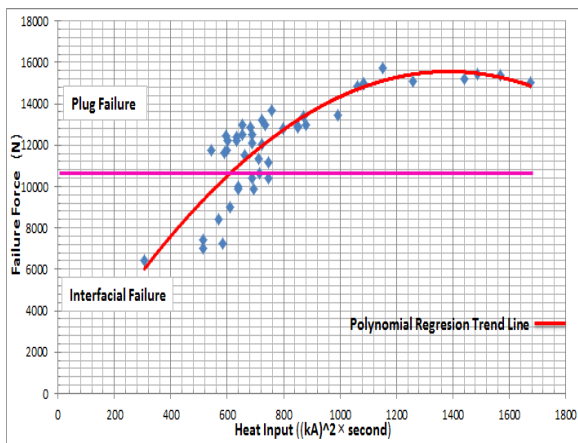


Fig. 22. input in the Maximum fracture loads versus welding energy tensile-shearing tests.

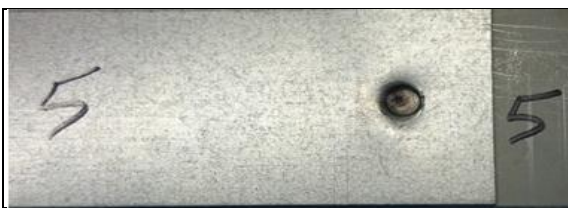


Fig. 23. Strong indentation due to high current input setup, Ex. No. 5.

### Numerical Simulations with SORPAS<sup>®</sup> 3-D

A significant advantage of simulation over experiment in RSW, which allows the engineer to monitor different physical and mechanical phenomena occurring during welding. 2-D Simulation by SORPAS<sup>®</sup> is quite sufficient with many cases. However, welding the sandwich sheet with other cover sheets and using a shunt

tool is not recommended to simulate with 2-D, since the case consider as a 3-D problems and this is in line with Nielson and et. al. [32 and 33]. Plenty effort has been conducted to simulate the case in 3-D SORPAS<sup>®</sup> by place the shunt as a third tool in the side end of the sheets for conducting electrical current between the cover sheets through the shunt connection, in addition of treating the polymer core in special input data as 2-D simulations. The meshes of the objects are shown in Fig. 24, which presents the details of the mesh allowing a reasonable discretization without a huge number of elements. The mesh is refined in welding zone to be able to simulate the necessary gradients. Besides mesh refinement, the elements are aligned strategically such that they follow the overall shape of the weld zone and in particular the contact zone defined by flat sheet round mesh.

After finding the optimum welding time and current (8-9 cycles, 5-5.5 kA) for the 1<sup>st</sup> pulse in numerical 2-D and practical experiments, using 3-D simulation to find the the optimum welding time and current for the 2<sup>nd</sup> pulse. A number of weld settings are simulated to show the influence of changing parameters.

Fig. 25 illustrates the current density, which indicates the current flow through shunt tool before the polymer core melted and squeezed out, i.e. the current does not flow through the contact area (proposed welding area).

Fig. 26 shows the process peak temperatures in the end of the weld time for simulated joint in sandwich steel with cover sheets for different weld settings (welding current and time). The images of the left part in this figure show the configuration with welding time setup equal to 2 cycles, this welding time is considered a very short time since there is no weld or bad shape nugget despite with high current (14 kA), which is considered very high value in the case of welding steel sheets with these thicknesses, see Fig. 26-d. While the images of the right part in this figure show the configuration with welding time setup of 6 cycles. With low welding current (6 kA) no weld is yet formed and just start forming with welding current of 7.32 kA and the weld nugget increase in size with increasing current, but with 10 kA the nugget is very large and is negatively affected welding quality and the whole process especially of adhesion the sheets with the electrodes, see Fig. 26-g. Therefore, the range of weldability is narrow with this welding time (6 cycles). One of the best weld setting simulations is 5 cycles in time and 9.54 kA in current that seems clear in the nugget size and shape as shown in Fig. 26-h.

Fig. 27 shows the simulated nugget compared with macro etched cross-section nugget spot welded for Ex. No. 23 with welding parameters 6.36 and 9.74 kA for current, 8 and 5 cycles for time. It can be seen that shape and size (4.7 mm) of the weld is predicted relatively a very fine fit with actual nugget as well as the HAZ zone.

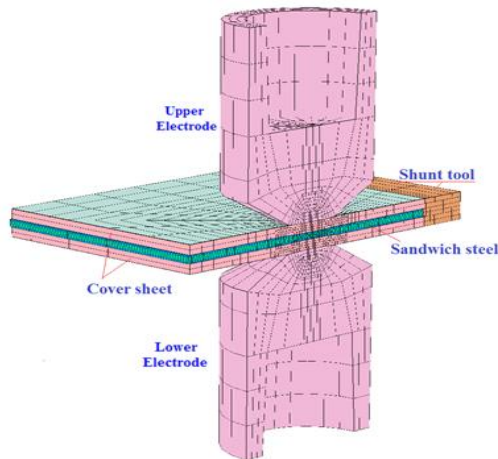


Fig. 24. Simulation mesh with 3-D SORPAS® for RSW Sandwich steel with cover sheets

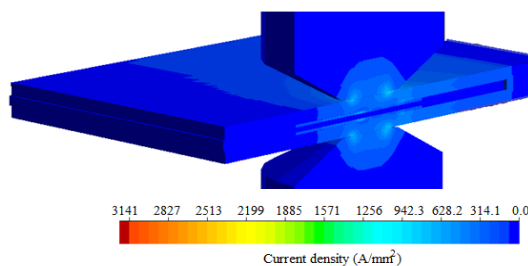


Fig. 25. Current flow through shunt tool.

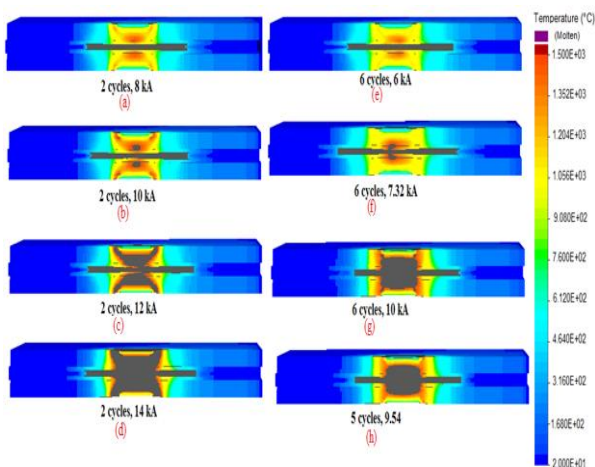


Fig. 26. Process peak temperatures in the end of the weld time for different weld settings.

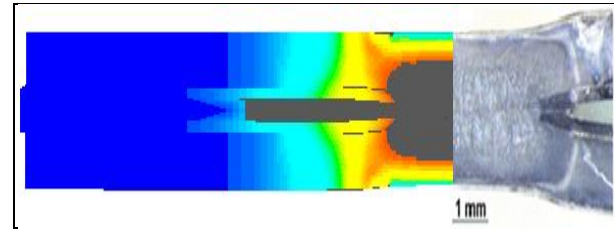


Fig. 27. Comparison between simulation and metallographic.

#### 4. Conclusions

This study proved the success of using resistance spot welding on sandwich steel (Litecor®) with DP800 cover sheets by using a copper shunt tool for resolving a non-conductivity problem of a polymer core. It was found that the weldability could be improved with using two pulses and optimized their welding parameters. The significant conclusions drawn from this numerical and experimental work are as follows:

1. It is required to be accurate where selecting the distance between the electrode and the shunt tool because it needs the shunt tool to be close as much as possible from the electrode before melting and squeezing out the polymer and to be far as much as possible after that, 19 mm distance is quite sufficient.
2. As energy (heat) input increased the nugget size increased. However, where it reached its critical value (about 6000 J) the nugget size did not increase as the same proportion due to the expulsion occurred.
3. The hardness in the fusion zone and HAZ was more than two times higher than that in the base metals due to the formation of new martensite.
4. The maximum fracture load of welded specimen in tensile-shearing test is about 15.5 kN corresponding with welding current RMS about 13 kA and welding time of 5 cycles. The failure mode is plug corresponding with more than 10 kN as fracture load, while less than this value failure is interfacial mode.
5. With increasing the current in 2<sup>nd</sup> pulse as more than RMS 14 kA, welding defects will occur such as large void and crack.
6. The optimum welding parameters are; 3.5 kN, (5.5 kA, 8 cycles), and (10 kA, 5 cycles) for the electrode force, welding current and time of first and second pulse respectively.
7. The existence of the new computer program, SORPAS® 3-D, provides the ability of simulating a variety of resistance welding cases such as this case that is not properly simulated by 2-D analysis.

## Acknowledgement

This work is part of project to host the author at Technical University of Denmark DTU as a postdoc. The author would like to thank Department of Mechanical Engineering at DTU, in particular Dr. Niels Bay and Dr. Chris Nielson and all colleagues at work. Special thanks to Wenqi Zhang, director of SWANTEC for supplying the license of SORPAS® program.

## 5. References

- [1] Mathers G., (2002), "The Welding of Aluminum and Its Alloys", Cambridge, United Kingdom: Woodhead Publishing.
- [2] Boomer D. R., Hunter J. A., and Castle D. R., (2003), "A New Approach for Robust High-Productivity Resistance Spot Welding of Aluminum", SAE Technical paper 1-0575.
- [3] Kim D. C., Park H. J., Hwang I. S., and Kang M. J., (2009), "RSW of Aluminum alloy sheet 5J32 Using SCR type and Inverter Type Power Supplies", *Int Sci J*; 38(1):55-60.
- [4] Al Naimi Ihsan K., Al Saadi Moneer H., Daws Kasim M., Bay N., (April, 2014), "Improving Resistance Welding of Aluminum Sheets by Addition of Metal Powder", *Proc IMechE Part L: Journal Materials: Design and Applications*(0) 1–10. <http://pil.sagepub.com/content/early/2014/04/28/1464420714533526.full.pdf?ijkey=xF9K VXDGqE4Ktzz&keytype=ref>.
- [5] Chao Y. J., (2003). Ultimate Strength and Failure Mechanism of RSW Subjected to Tensile, Shear, and combined tensile/Shear Loads. *ASME J. of Engineering Materials and Technology*, Vol. 125, 125-13.
- [6] Cho W., Li and Hu, (2006). Design of Experiment Analysis and Weld Lobe Estimation for Aluminum Resistance Spot Welding. Supplement to the *Welding Journal*, sponsored by the American Welding Society and the Welding Research Council.
- [7] Brown D. J., Newton, C. J., and Boomer, D., (1995). Optimization and Validation of a Model to Predict the Spot Weldability Parameter lobes for Aluminum Automotive Body Sheet. *Advanced Technologies & Processes*, IBEC, pp. 100-106.
- [8] Nielson C.V., Fris K.S., Zhang W., Bay N., (2011). Three-Sheet Spot Welding of Advanced High-Strength Steels. *Welding Journal*, Vol. 90 pp. 32s-40s.
- [9] RWMA, (2003). Resistance Welding Process. *Resistance Welding Manuals*, printed by George H. Buchman, Nj. USA.
- [10] Gustafsson R. N., (2000). Sandwich construction. *Proc. 5th International Conf. Zurich*, Emas publishing, pp. 169-176.
- [11] Akihiko Nishimoto, Yukichi Watanabe, Yasushi Fujii, Shinji Kabasawa, and Yasunori Matsuda, (1988). *Weldable Vibration Damping Steel*. NKK Technical Review No. 53.
- [12] Fukui, and Taka, (1989). development of direct spot weldable damping sheet. *Sumitomo metals*, pp. 111-118.
- [13] Tanaka, and Sato, (1989). Spot weldability of the vibration damping steel sheet. *ISIJ*, pp. 230-236.
- [14] Fujii, and Uwai, (1993). Development of vibration damping steel sheet using thermosetting resin. *SAE technical Paper Series*, Int. Congress and Exposition.
- [15] Markaki A. E., Westgate S. A., and Clyne T. W., (2002). The stiffness and weldability of an ultra-light steel sandwich sheet material with a fibrous metal core. *Processing and Properties of Lightweight Cellular Metals and Structures*, TMS, 15-24, Seattle.
- [16] Senkara, J., Zhang, H., and Hu, S. J., (2004). Expulsion Prediction in Resistance Spot Welding. *Welding Research, Welding Journal*, pp. 123-132.
- [17] Oberle H., Commaret C., Magnaud R., Minier C., and Pradere G., (1998). Optimizing Resistance Spot Welding Parameters for Vibration Damping Steel Sheets. *Welding research Supplement, Welding Journal*, pp. 8-s to 13-s.
- [18] Tan J. C., Westgate S. A., and Clyne T. W., (2007). Resistance welding of thin stainless steel sandwich sheets with fibrous metallic cores: experimental and numerical studies. *Science and Technology of Welding and Joining Journal*, Vol. 12, No 6, pp. 490-504.
- [19] Hoffmann, Oliver, (2012). *Steel Lightweight Materials and Design for Environmental Friendly Mobility*. ThyssenKrupp Steel Europe Catalogue, Aarus.
- [20] Zhang W., Chergui A., and Nielsen C. V., (September 2012). Process Simulation of Resistance Weld Bonding and Automotive Light-weight Materials, *Proc. 7th International Seminar on Advances in Resistance Welding*, Bosan Korea.
- [21] LITECOR® (August-2014), The intelligent solution for cost-effective lightweight design,
- [22] ISO 14273:2000(E), "Specimen dimensions and procedure for shear testing resistance

- spot, seam and embossed projection welds", Licensed to SWANTEC.
- [23] ISO 5821: (2009), "Resistance welding — Spot welding electrode caps", Licensed to SWANTEC, ISO Store order #: 10-1067232.
- [24] SCHMIDT & BITTNER, (2011), "Electrode Caps-1", [www.wma-sb.de](http://www.wma-sb.de)
- [25] SAAB-Swedish Steel, "Dogal 600 and 800 DP", [www.ssab.com](http://www.ssab.com)
- [26] Pieronek, D., Böger, T., Röttger, R., (Oct. 2012). Modeling Approach for Steel Sandwich Materials in Automotive Crash Simulations. ThyssenKrupp Steel Europe.
- [27] SWANTEC Software and Engineering ApS. SORPAS®, Version 11.6.
- [28] Ma, C., Chen, D. L., Bhole, S. D., Boudreau, G., Lee, A., and Biro, E., (2008). "Microstructure and fracture characteristics of spot-welded DP600 Steel", *Materials Science and Eng. A* 485, PP. 334-346.
- [29] Pouranvari, M., (2010). "Prediction of Failure Mode in AISI 304 Resistance Spot Welds", *Association of Metallurgical Engineers of Serbia*, UDC: 621.791.763, PP. 23-29.
- [30] Tsipourid, P., (2006). Mechanical Properties of Dual-Phase Steels. PhD thesis submitted to Technical University of Munich, Germany.
- [31] Pouranvari, M., and Ranjbarnoode, E., (2011). Resistance Spot Welding Characteristic of Ferrite-Martensite DP600 Dual Phase Advanced High Strength Steel-Part III: Mechanical Properties. *World Applied Sc. Journal* 15 (11): 1521-1526.
- [32] Nielson, C. V., Zhang, W., Martins, P. A. F., and Bay, N. (2015). 3D numerical simulation of projection welding of square nuts to sheets. *Journal of Materials Processing Technology* 215, PP. 171–180.
- [33] Nielson, C. V., Zhang, W., Perret, W., Martins, P. A. F., and Bay, N. (2014). Three-dimensional simulations of resistance spot welding. *Proceedings of the Institution of Mechanical Engineers, Part D: Journal of Automobile Engineering*, I-13.

## قابلية اللحام لمادة جديدة من صفائح الفولاذ المركب لتطبيقات المركبات

إحسان كاظم عباس النعيمي

التعليم المهني/ وزارة التربية

البريد الإلكتروني: [ihsan\\_kad@yahoo.com](mailto:ihsan_kad@yahoo.com)

## الخلاصة

يواجه العالم اليوم أزمة في الطاقة بسبب الزيادة المستمرة لاستهلاك الوقود نتيجة تعاظم الطلب على جميع أنواع المركبات إن هذه الدراسة هي واحدة من الجهود التي لها علاقة بتقليل وزن المركبات باستخدام مادة جديدة من الفولاذ المركب، وتتكون هذه المادة من طبقتين رقيقتين من الفولاذ وسطهما (في القلب) مادة بوليمر. يمكن تنفيذ لحام المقاومة النقطي على المعادن بسهولة، ومع ذلك فقد تم تصميم قطعة نحاسية لتحويل التيار الكهربائي لحل مشكلة عدم التوصيل الكهربائي للبوليمر ولإتمام تنفيذ لحام المقاومة الكهربائية على الفولاذ المركب مع صفائح أخرى من الفولاذ نوع DP800 عالي المقاومة. أجريت المحاكاة العددية بوساطة  $SORPAS^{\circledR}3D$  لاختبار قابلية اللحام لهذه المادة الجديدة ودُعِمَت النتائج بعدد من التجارب العملية تم التوصل إلى الاستنتاج الآتي لهذا البحث، إن قابلية اللحام يمكن تحسينها باستخدام نبضتين من اللحام وتثبيت أفضل متغيرات عملية اللحام لهاتين النبضتين أجريت اختبارات القص- الشد لتقويم قوة الصفائح الملحومة. تم أيضاً تحليل الصور المجهرية والمرئية (غير المجهرية) التي التُقِطت بالميكروسكوب الضوئي وبالماسح الإلكتروني مع التحليل الطيفي لمنطقة اللحام وإجراء المقارنة لتلك المنطقة مع متغيرات عملية اللحام المختلفة، واستنتجت المتغيرات المثلى التالية: قوة ضغط أقطاب اللحام ٣.٥ كيلو نيوتن، التيار الكهربائي وزمن اللحام هي (٥.٥ كيلو أمبير، ٨ دورات) و (١٠ كيلو أمبير، ٥ دورات) لنبض اللحامين الأول والثاني على التوالي